Tailored WBGT as a heat stress index to assess the direct solar radiation effect on indoor thermal comfort

Shayan Mirzabeigi[a], Behrooz Khalilinasr[b], Andrea G. Mainini[b], Juan D. Blanco Cadena[b], Gabriele Lobaccaro[c]

[a] Department of Sustainable Resources Management, State University of New York College of Environmental Science and Forestry, Syracuse, NY, USA

[b] Department of Architecture, Built Environment and Construction Engineering, Politecnico di Milano, Milan, Italy

[c] Department of Civil and Environmental Engineering, Faculty of Engineering, Norwegian University of Science and Technology, Trondheim, Norway

Abstract

Uncontrolled solar radiation and the related effects on occupant productivity can lead to considerable indoor thermal discomfort in office environments. In this paper, the Radiance Daylight Coefficient (DC) method is used to assess incoming solar radiation and consequent indoor thermal discomfort through delta mean radiant temperature (ΔMRT). The ΔMRT allows expressing an adjusted predicted mean vote (Adjusted PMV). Under the conditions of direct solar radiation, the Adjusted PMV value surpasses the applicability range of the standard PMV in terms of MRT value. To overcome this limitation, the assessment of the effect of incoming shortwave solar radiation is expressed in the heat stress index of wet bulb globe temperature (WBGT). This procedure was tested under a variety of climatic conditions (e.g., Sol-air temperature) to estimate dissatisfaction in indoor office environments located in Milan (Italy) for an occupant positioned at different distances from the fenestration (0.75 m, 1.25 m, and 1.75 m) and exposed to direct solar radiation (e.g., without shading devices). The condition with no shading device was then compared with the condition with shaded glazing to test the impact of the solar radiation on the indoor thermal stress conditions. The results reported through ΔWBGT allow the estimation of the heat stress conditions on an annual basis when ΔWBGT > 0. Finally, it is proposed that the metric of Annual Radiation Heat Stress (ARHS) should include ΔWBGT and assess the heat stress spatially due to the incoming direct solar radiation.

Keywords

Indoor thermal comfort; Solar radiation; Radiance DC method; WBGT.

Nomenclature

Adjusted MRT: adjusted mean radiant temperature (°C)

Adjusted PMV: adjusted predicted mean vote (-)

ARHS: annual radiation heat stress (%)

CAV: clothing adjustment value (°C)

C_p: specific heat capacity at constant pressure (J/kg K)

ERF: effective radiant field (W/m^2)

E_{solar}: total shortwave solar radiant flux (W/m^2)

f_{eff}: fraction of body exposed to sun (-)

h_r: radiation heat transfer coefficient (W/m^2K)

I_{cl}: thermal insulation index (clo)

i_m: permeability index (-)

M: metabolic rate (W)

MRT: mean radiant temperature (°C)

PMV: predicted mean vote (-)

PPD: predicted percentage of dissatisfied (%)

p_v: water vapor pressure (Pa)

RH: relative humidity (%)

T_a: air temperature (°C)

T_c: cooling set point (°C)

T_g: black globe temperature (°C)

T_h: heating set point (°C)

T_{nwb}: natural wet bulb temperature (°C)

T_{pwb}: psychrometric wet bulb temperature (°C)

T_{sol}: solar transmittance (-)

U: thermal transmittance (W/m^2K)

v: air speed (m/s)

WBGT: wet bulb globe temperature (°C)

$WBGT_{eff}$: effective wet bulb globe temperature (°C)

$WBGT_{LW}$: longwave wet bulb globe temperature (°C)

$WBGT_{ref}$: reference wet bulb globe temperature (°C)

$WBGT_{SW}$: shortwave and longwave wet bulb globe temperature (°C)

x: the thickness of assigned element (m)

α_{LW}: longwave radiation absorptivity (-)

α_{SW}: shortwave radiation absorptivity (-)

ΔMRT: delta mean radiant temperature (°C)

ΔWBGT: delta wet bulb globe temperature (°C)

λ: thermal conductivity (W/mK)

ρ: thermal density (kg/m^3)

ρ_{sol}: reflectance (-)

1 Introduction

In many parts of the world humans commonly spend most of their life indoors, and the majority of the population of the world works in an office-like layout setting [1]. As such, it is beneficial to better analyze the indoor office environment, especially thermal comfort, which is known to impact occupants productivity [2] and well-being [3]. Thermal comfort could be expressed as a condition under which the user perceives satisfaction with the perceived thermal environment [4]. This condition is not only affected by objective quantitative variables, but also subjective qualitative ones related to the habits of the user [1]. Delivering and/or maintaining overall thermal comfort in a building is often a complex task. Multiple environmental parameters (e.g., air temperature, surface temperature, relative humidity, mean radiant temperature, wind speed, and direction) and other geometrical and physical factors(e.g. window location, orientation and dimensions, occupants clothing, user activity, position, and mood), have been proven to strongly affect the thermal comfort perception of occupants [1]. The parameters directly related to the building users differ per individual due to different factors (e.g. age, sex, metabolic rate) [5].

The first instrumental work in the area of thermal comfort and occupants perception was performed by Fanger (1970) [6]. He introduced an analytical model to estimate thermal comfort perception that combines physiological parameters with human behavior variables to define the two synthetic comfort indices as the predicted mean vote (PMV) and the predicted percentage of dissatisfied (PPD) [7], which is the proportion of people dissatisfied with the thermal conditions in indoor environment, considering it too warm or too cold [7]. Fanger's thermal comfort model (PMV model) was based on subjective surveys and rigorous experiments involving subjects wearing different levels of clothing and engaging in different levels of activity who were exposed to different steady-state

conditions in a controlled indoor environment. This model is generally applied when it is necessary to estimate the predicted thermal comfort condition of a mechanically heated, cooled, or ventilated indoor space.

However, researchers have found that when this model is applied for a building without mechanical systems, it is inaccurate in predicting the occupant's thermal discomfort. The results showed that PMV could underestimate the thermal sensation by up to 13% in summer and overestimate it by up to 35% in winter within naturally ventilated buildings [8].

De Dear and Brager (1998) [9] have stated that occupants have a positive attitude towards adapting to the environmental conditions, which was not considered during the development of the PMV model. De Dear and Brager proposed an alternative approach, known as the adaptive comfort model. This approach was based on field experiments and analysis of human acceptability of a thermal environment that considered adaptive behavior, physiological and psychological adjustments [9]. Similar approaches have been recalled in ASHRAE-55 [4] and EN-16798 [10].

Among the environmental conditions, ambient temperature and humidity ratio play a decisive role in the occupants' thermal comfort. However, solar radiation falling over the user's body is also one of the most influencing variables that contribute to shaping the perceived thermal sensation of a user in an indoor space [11]. In that regard, solar radiation requires deeper analysis and more consideration due to its influence on the thermal perception of feeling warmer, which can subsequently have negative impacts on occupants' productivity [12]. Therefore, it is fundamental to consider the effect of shortwave solar radiation on the occupant's indoor thermal comfort.

This research is motivated to provide a new perspective in assessing the effect of incoming shortwave solar radiation falling over the occupants and in estimating the indoor thermal comfort. To that end, by exploiting its lower sensitivity to strong variations of the adjusted mean radiant temperature (Adjusted MRT) perceived by the user, the possible application of the heat stress index of wet bulb globe temperature (WBGT) is considered as an alternative for the PMV model.

Studies using the WBGT approach have assessied the thermal comfort in an indoor environment, especially working environments with hot working conditions However, the study presented here focuses on the Delta Value approach. Its novelty is based on the implementation of a modified version of the WBGT for indoor thermal comfort assessment, evaluated using the Radiance's Daylight Coefficient (DC) method, a parametric and climate-based approach, which allows the inclusion of the shortwave contribution of the solar radiation over the human body.

Section 2 (Background) presents the state-of-the-art of the research field framing this study. Section 3 (Methodology) defines the computer-aided simulation workflow and describes the procedure for calculating the modified version of WBGT. The description includes the metric Annual Radiation Heat Stress (ARHS) to assess the heat stress spatially due to the incoming direct solar radiation. Next, s Section 4 (Results and discussion) presents the outcomes of the simulation and their discussion through graphics (e.g., false-color plots) and analytically using the proposed metrics (i.e. WBGT, ΔWBGT:). The Section 5highlights and discusses the main limitations of the study. Finally, Section 6 (Conclusions) summaries the study and the most significant outcomes.

2 Background

2.1 The effects of shortwave solar radiation on users' perception of thermal comfort

Uncontrolled direct solar radiation flux often causes significant visual (e.g., glare) and thermal (e.g., overheating, cooling load) issues, especially in buildings with unshaded glazing [12]. International standards ISO-7730 [7] and EN-16798 [10], which are mainly based on a generic radiosity approach, do not include shortwave radiation when calculating comfort. However, shortwave solar radiation could be the most substantial component of total solar radiation gathered indoors [13]. Although direct solar radiation is considered in every dynamic simulation, the analysis of the effect of solar radiation directly falling on the occupant is neglected in different comfort models. It is also necessary to underline that when the uncontrolled direct solar radiation falls on the occupants, it can also influence peak energy loads, such as an increased energy consumption resulting from the need of users to mitigate the perceived thermal condition by using building systems [14].

Complex human models have been elaborated and proposed that allow designers and modelers to estimate the body core and skin temperature of the occupant based on the surrounding thermal environment. Skin temperatures can then be used to determine local thermal sensation as input for comfort assessment [14], [15]. In addition, there are models relying on equivalent temperature values or advanced thermal comfort models, like the one presented by the University of California Berkeley [12], [16], that can be used to predict human comfort in transient, non-uniform thermal environments.

In the case of direct solar radiation falling on the occupant, ASHRAE-55 [4] introduces two approaches for dealing with this issue when determining the thermal comfort condition [17]: (1) the prescriptive approach, which is applicable only when specific criteria are met (see Appendix C in [4]). It asserts that when these conditions arise, a mean radiant temperature (MRT) increase of 2.8 °C (higher than average air temperature) can be used. (2) the performance approach, based on the work of Arens et al. [12], which calculates Adjusted MRT by summing up

147 the contributions of the calculated longwave and shortwave MRT.. Under these conditions, MRT depends on solar
148 radiation distribution, surrounding context, direct and indirect solar transmittance of the fenestration system,
149 occupant position and posture, body exposure, sun position, irradiance value, and clothing absorptivity.
150 A limitation of the performance approach method is that the incoming direct and diffuse solar radiation considers
151 a fixed fraction of the sky vault and a projected area of the person exposed to radiation for static scenarios [14].
152 The point-in-time results can also lead to an inaccurate understanding of the performance of the fenestration
153 systems, especially in the case of solar shading systems that are considered to manage solar radiation flux for the
154 whole year [14].
155 As reported in [14], by applying the Radiance ray-trace method and DC method, the intensity of total solar
156 radiation falling on the occupant's body can be estimated on an annual basis, with the aim of predicting the
157 differences in indoor thermal comfort of occupants.
158 Zani et al. (2019) [17] introduced the Annual Discomfort Radiation index (ARD index) to spatially assess the
159 discomfort caused by solar radiation. This index shows areas on the floor plan that represents uncomfortable
160 thermal conditions. It works by mapping the variation of delta mean radiant temperature (ΔMRT) [17], and it is
161 based on the concept of an annual metric like Daylight Autonomy (DA) [18].

162 ## 2.2 Comfort conditions assessment considering the shortwave solar radiation

163 The PMV equation uses four environmental variables: air temperature (T_a), mean radiant temperature (MRT), air
164 speed (v), relative humidity (RH); and two subjective variables: clothing thermal insulation index (I_{cl}) and
165 metabolic rate (M). It predicts thermal sensation ratings of occupants on the ASHRAE seven-point thermal
166 sensation scale [7]. Based on ISO-7730 [7], these values are required to be within a valid range when computing
167 PMV, which are: "M: 0.8 to 4 met, I_{cl}: 0 to 2 clo, T_a: 10 to 30 °C, MRT: 10 to 40 °C, v: 0 to 1 m/s, P_v: 0 to 2700
168 Pa".
169 The variations between reported and predicted thermal sensation have been attributed to errors in measurements,
170 which relate to inaccuracies in the input parameters required for calculating PMV, especially in assessing the
171 average clothing insulation values and metabolic rate. Errors have also been associated with contextual effects
172 [19]. The PMV model is based on experimental environments (e.g., climate chamber), that require a more in-
173 depth study, as stated by Beizaee et al. (2012), [19] in comparison to the occupant's usual environmental settings.
174 The PMV model is certainly the most widely used and accepted thermal comfort index but needs to be more robust
175 to increase its applicability. Extreme conditions (e.g., those where the occupant is under direct solar radiation)

often cause the PMV rating to go beyond the seven-point thermal sensation scale (mainly above +3) due to Adjusted MRT values that exceed the MRT validity range. The interpretation of these results is rather uncertain since cases of PMV > +3 were not described within Fanger's model (i.e. no information on the degree of warmth perceived). Solving this issue could also enable the analysis of outdoor environments with the same procedure.

The CBE Thermal Comfort Tool includes both ASHRAE-55 and EN-16798 for its comfort calculation [20], [21]. An example is shown in Figure 1 using this tool [21] under EN-16798 settings. It displays the calculation for a time of the year for ASHRAE BESTEST in Milan (with ERF value of 91.0 W/m^2). The value of MRT, without the contribution of shortwave solar radiation, is estimated to be 28.0 °C, which corresponds to a PMV of 0.5 (Figure 1a). Under the same scenario, considering an adjustment in MRT due to solar radiation results in a condition of Adjusted MRT equal to 49.8 °C, which corresponds to a PMV of 4.4 (Figure 1b). The PMV increases 3.9 points when the shortwave contribution of solar radiation is considered. However, the Adjusted MRT value surpasses the applicability range due to the fact that it does not comply with the standard; in that regard, none outcome is obtained from the CBE Thermal Comfort Tool..

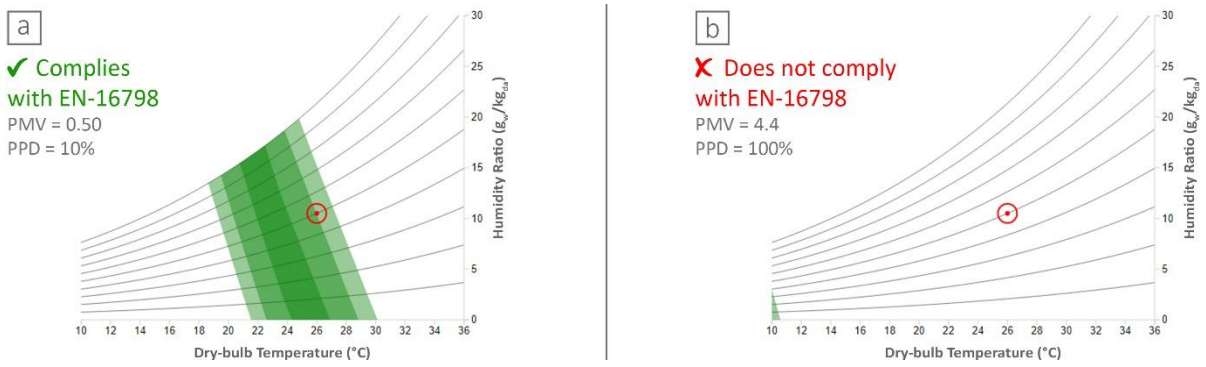

Figure 1 - Example of using the CBE Thermal Comfort Tool under EN-16798 (visualization with psychrometric chart) to compare predicted PMV: a) without solar radiation, and b) with solar radiation (under apparent comfortable conditions of T_a =26 °C, v =0.1 m/s, RH =50.0%, I_{cl} =0.6 clo and M =1 met).

2.3 Evaluation of solar radiation effects under proper heat stress index

The most important aspect of considering shortwave solar radiation as a cause of local discomfort is related to the methodology used to assess the caused dissatisfaction. Scenarios with direct solar radiation flux that carry large amounts of shortwave radiation and change occupant thermal comfort perception are not unusual, and the current definition of the PMV model provides a certain degree of uncertainty in which, for certain climatic conditions and room location, it is not possible to adequately assess or rate the thermal environmental perception.

In this study, solar radiation has been introduced as a heat stress phenomenon that can cause dissatisfaction for occupants both indoors and outdoors. To do so, heat stress is expressed through a suitable index. The effect of architectural design on outdoor thermal comfort is also unavoidable, and it is rare to find tools and methods that allow the evaluation of thermal comfort for both indoor and outdoor spaces [22]. The present study improves the evaluation of indoor comfort by taking into account influencing outdoor parameters (e.g., airspeed, ventilation, urban morphology, finishing materials, surface temperature, shortwave solar radiation), which could help to assess the dissatisfaction caused by shortwave solar radiation and ease the management of indoor discomfort in preliminary design stages. The focus of this study is to consider the solar radiation that significantly influences the MRT and consequently the comfort conditions.

The environmental thermal aspect constitutes a relevant issue related to human health and well-being. It comprises both heat-exchange conditions (i.e. stress) and the physiological responses (i.e. strain) [23], [24]. The heat stress indices are useful to understand the effects of the thermal environment on the thermal perception of humans [25]. Zamanian et al. (2017) [24] compared different thermal indices such as Wet bulb globe temperature (WBGT), Universal thermal climate index (UTCI), Subjective temperature index (STI), Predicted heat stress (PHS), and Humidex. Moreover, they shared the concern of potential risks of working in a hot environment related to physiological responses, or strain, such as a change in skin and core body temperature and heart rate. The association of thermal indices with some physiological parameters such as blood pressure, pulse rate, and skin temperature were studied by Zamanian et al., and based on the results of linear regression analysis, a significant correlation was found between skin temperature and WBGT. However, the results showed no significant relationship between physiological response and other thermal stress indices such as UTCI, PHS, STI, and Humidex [24].

Therefore, the WBGT was chosen as a proper heat stress index because (1) its versatility allows it to be applied in both indoor and outdoor comfort analysis; (2) solar radiation is a phenomenon that is firstly sensed by the skin, and there is a strong link between the WBGT and skin temperature. Consequently, the WBGT allows a more reasonable assessment of the thermal dissatisfaction caused by the contribution of the solar radiation and it leads to defining new ways to control thermal discomfort.

3 Methodology

In this work, the heat stress index of WBGT is implemented to overcome the existing limitations of PMV and Adjusted PMV in considering the effect of solar radiation. When the outcome of Adjusted PMV is beyond the

model's reliability, this heat stress index can mitigate the impact of extreme events. The use of the Radiance DC method on the Grasshopper platform allows the calculation of the hourly incident solar radiation landing on the human body. The elaboration of a script on the Grasshopper platform allows the detailed and spatial estimation of the WBGT affected by the solar radiation and the comparison with the different thermal stress indices

3.1 The simulation framework

In this Section the workflow is presented to introduce the Adjusted MRT in the calculation procedure for the WBGT and explain how to post-process the results in order to introduce a spatial and climate-based thermal perception index. The Adjusted MRT predicts the variation of the heat stress of occupants due to the solar radiation across the floor plan to be predicted and the total discomfort hours to be evaluated.

A climatic based workflow is used to evaluate the effect of direct solar radiation on human thermal comfort across indoor spaces for one year. The workflow is based on validated simulation engines, Radiance for daylight and solar radiation analysis and Energy Plus for energy analyses through Ladybug Tools, to conduct simulations in in the Grasshopper environment. This approach represents an alternative to the method of ASHRAE-55 (appendix C) by calculating the WBGT heat stress index.

The workflow allows the calculation of the annual hourly values of total radiation (e.g., direct, reflected, and diffuse) on the human body with the Radiance DC method and, subsequently, ERF, ΔMRT, and the consequent value of ΔWBGT. The analysis conducted in the Grasshopper platform allows the automatizing of the workflow for multiple annual simulations. It is tested for an occupant placed at different distances from the fenestration and exposed to direct solar radiation and computes the degree of heat stress in an indoor environment.

Based on this procedure, the Annual Radiation Heat Stress metric (ARHS), as a modified climate-based index, is presented to assess spatially extreme heat stress conditions. Moreover, the methodology is tested to provide information on how well a fenestration system performs in controlling the incoming solar radiation, in terms of occupants' thermal comfort, and estimating the heat stress caused by the solar radiation during the year in an office environment.

As shown in Figure 2, the simulation workflow is divided into six parts. In Section 3.1.1, the Rhinoceros scene and manikin modeling are described. Section 3.1.2 describes the Radiance DC method. Thanks to this method, the hourly intensity of solar radiation that is transmitted through the fenestration system and lands on the human body is calculated. Then, Section 3.1.3 briefly explains the Energy Plus simulation to calculate the air temperature, relative humidity, surface temperatures, airspeed, and longwave MRT. Section 3.1.4 introduces the procedure to calculate the delta mean radiant temperature value. In Section 3.1.5, the calculation of WBGT is described.

Finally, Section 3.1.6 explains the spatial mapping and the ARHS to assess heat stress due to the incoming direct solar radiation.

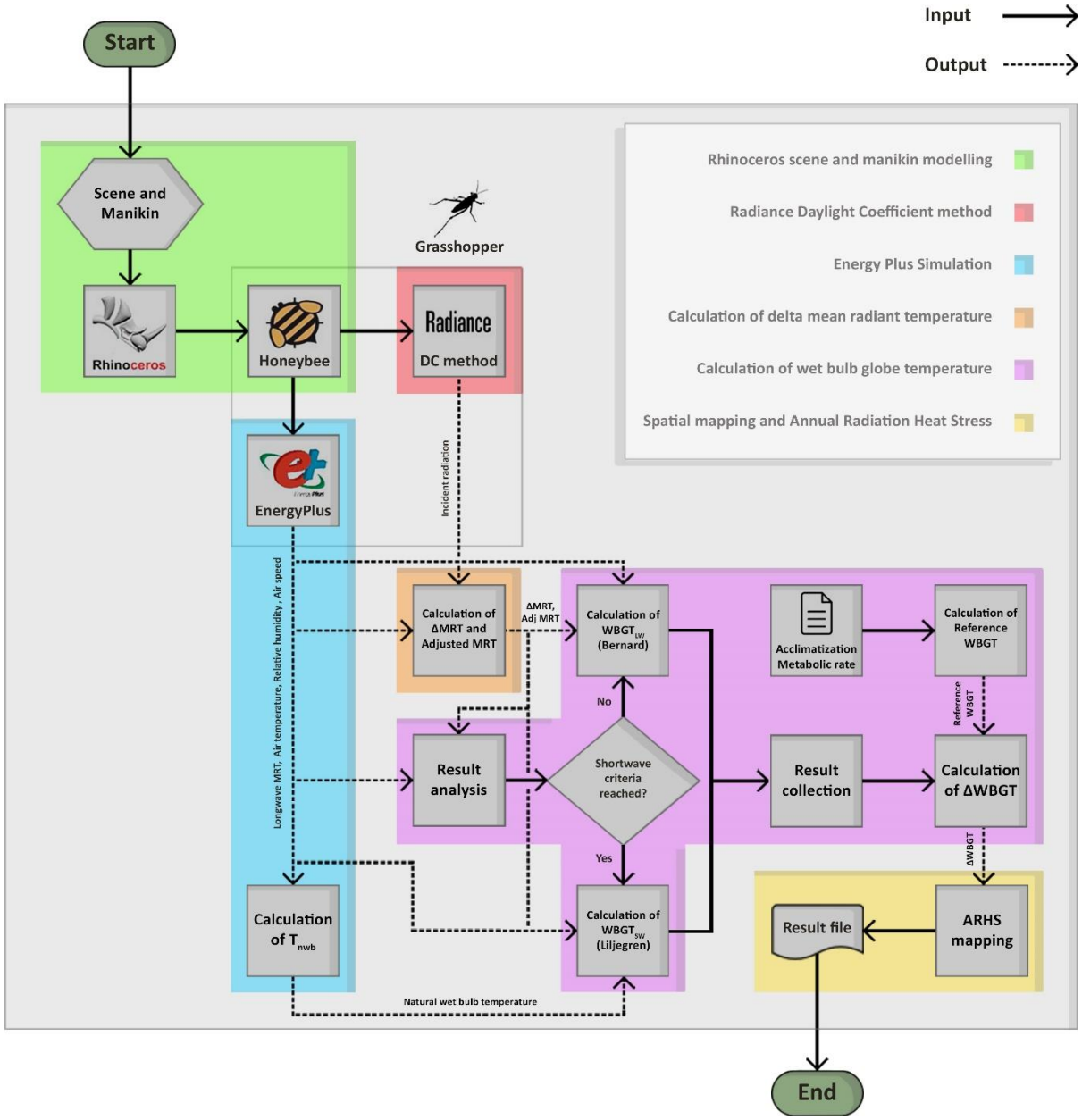

Figure 2 - Simulation workflow for indoor thermal comfort analysis. The six main parts have been clustered and differentiated with colors.

3.1.1 Rhinoceros scene and manikin modelling

Rhinoceros geometry information is created and handled via Grasshopper visual language [26]. Honeybee plug-in within Ladybug tools is used to generate the input text files for Radiance and Energy Plus simulations. The manikin is constituted by 133 planar mesh faces to calculate the total solar radiation falling on each manikin's body.

3.1.2 Radiance Daylight Coefficient method

The DC method described by Zani et al. (2018) [14] is used in the simulation workflow to compute the incoming solar radiation falling on the manikin. The DC (Two-Phase) method includes the calculation of the Daylight Coefficient matrix, considering sky conditions and scene characteristics, and sky vector (matrix), based on direct and diffuse solar radiation. The next step, after identifying matrices, is matrix multiplication to compute the irradiance value. Incident solar radiation is then calculated for each face mesh of the manikin, for each hour of the year. This process is repeated for each manikin's location in the room scene, described later in chapter 3.2.

3.1.3 Energy Plus simulation

The geometrical data in Rhinoceros is transferred into an IDF text file. The Energy Plus engine is used for the calculation of the air temperature, relative humidity, surface temperatures, and longwave MRT in the room. The longwave MRT is calculated considering the surface temperatures of walls, glazing surfaces, and the corresponding view factor for the exact user position. These values are later used to calculate the WBGT.

3.1.4 Calculation of delta mean radiant temperature

The solar radiation falling over the manikin, discretized in polygonal patches, is then transformed into the ERF and shortwave ΔMRT, which reflects the potential increase of MRT caused by the solar radiation [12] for a person exposed to solar radiation in the indoor environment (see equations (1) and (2)). These measures are both mainly affected by the solar absorbance of the human skin, and the percentage of the exposed surface of the body and the incident solar radiation.

$$\mathrm{ERF} = \frac{\alpha_{\mathrm{SW}}}{\alpha_{\mathrm{LW}}} \mathrm{E}_{\mathrm{solar}} \quad (1)$$

$$\Delta\mathrm{MRT} = \frac{\mathrm{ERF}}{\mathrm{f}_{\mathrm{eff}} \mathrm{h}_{\mathrm{r}}} \quad (2)$$

3.1.5 Wet bulb globe temperature calculation methods

The WBGT is defined as a heat stress index, and it is a screening method for the presence or absence of heat stress described in the ISO-7243 [27]. The level of heat stress is dependent on the heat transfer between the body and the surrounding ambient environment, the heat production inside the human body as a result of physical activity, and the clothing worn, which alters the heat exchange, I_{clo}.

Furthermore, the same standard [27] states that the WBGT is calculated based on the measured natural wet bulb temperature (T_{nwb}) and black globe temperature (T_g), considering direct solar radiation, either outdoors or indoors. The weighting of the global temperature is reduced by the air temperature (T_a); thus, to compute WBGT, eq. (3)

is proposed when only the longwave solar radiation is considered, while eq. (4) can be used when both long and shortwave solar radiation are included.

$$WBGT_{LW} = 0.7\,T_{nwb} + 0.3\,T_g \quad (3)$$

$$WBGT_{SW} = 0.7\,T_{nwb} + 0.2\,T_g + 0.1T_a \quad (4)$$

The calculation of WBGT is performed by assuming standard and fixed work clothing (I_{cl}=0.6 clo, i_m=0.38) for an average clothing condition [27]. To consider the effect of actual clothing other than standard work clothing in the calculation of the WBGT, its value can be calculated by the clothing adjustment value (CAV). The result is called Effective wet bulb globe temperature ($WBGT_{eff}$), which is an estimation of the heat stress of the actual clothing used as an equivalent environment [27], and it can be computed according to the eq. (5).

$$WBGT_{eff} = WBGT + CAV \quad (5)$$

The $WBGT_{eff}$ values are computed with eq. (1) or (2), and (3), which are then compared with Reference WBGT ($WBGT_{ref}$) values to estimate the heat stress conditions. Figure 3 shows that the $WBGT_{eff}$ value is compared with $WBGT_{ref}$ value, and the result will be delta wet bulb globe temperature (ΔWBGT). There will be heat stress conditions if ΔWBGT is positive, in which case it would be important to directly mitigate the heat stress [27]; otherwise, there will be a condition without heat stress.

The $WBGT_{eff}$ depends on the concept of acclimatization, which is defined based on the ISO-7243 [27]. Acclimatization occurs when a person is exposed to hot working conditions for at least seven days before the analysis period. If this is not the case, the person will be in a non-acclimatized condition.

Figure 3 also shows the relationship between metabolic rate and $WBGT_{eff}$ (with standard work clothing). The straight line shows the limit of acceptable heat stress exposure for normal, healthy, acclimatized workers, and the dashed line represents a sustainable level of heat stress exposure for normal, healthy, non-acclimatized workers, where 115 W < M < 520 W. For acclimatized people, eq. (6) can be applied, while for non-acclimatized people, eq. (7) is included in the standard [27].

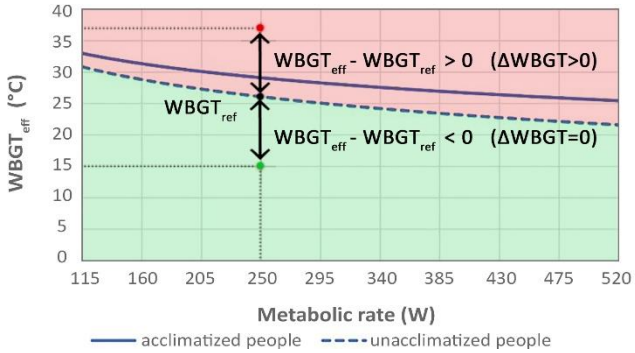

Figure 3 - Example comparison of $WBGT_{eff}$ and reference value limits by the metabolic rate (eq. (6) and (7) are used to draw $WBGT_{ref}$ lines from ISO-7243 [27]*).*

$$\mathrm{WBGT_{ref}} = 56{,}7 - 11{,}5 \log_{10}(\mathrm{M}) \quad (6)$$

$$\mathrm{WBGT_{ref}} = 59{,}9 - 14{,}1 \log_{10}(\mathrm{M}) \quad (7)$$

Table 1 shows the classification of levels of metabolic rate, including resting, low, moderate and high metabolic rates. In the section of Results, different outcomes are rendered based on the defining $WBGT_{ref}$ values concerning this classification of levels of metabolic rate.

Table 1 - Classification of levels of metabolic rate extracted from [28] *and corresponding $WBGT_{ref}$ values of the acclimatized and not-acclimatized person.*

Class	**M (W)**	**$WBGT_{ref}$ (°C) for acclimatized person**	**$WBGT_{ref}$ (°C) for non-acclimatized person**
0: Resting	115 (100 - 125)	33.00	30.84
1: Low metabolic rate	215 (125 - 235)	29.88	27.01
2: Moderate metabolic rate	300 (235 - 360)	27.97	24.67
3: High metabolic rate	415 (360 - 465)	26.59	22.99

ISO-7243 [27] set specific requirements for the globe and natural wet bulb thermometer measurements for the estimation of the WBGT index following the method presented in [29]. It is essential to understand if the WBGT can be calculated from meteorological measurements [30] and if it is possible to exploit the environment assessment databases available in the literature in which the mentioned parameters are provided [29].

Bernard and Pourmoghani [31] compared indoor measurements with calculated longwave wet bulb globe temperature ($WBGT_{LW}$). Their approach includes all meteorological variables as required by the WBGT calculation and the uses heat exchange principles and measurements (of a wetted wick) for T_{nwb} [30], [31]. The equations presented in Table 2 are used to calculate the T_{nwb} and not the WBGT. Unfortunately, their approach does not involve estimating the temperature of the black globe directly exposed to sun rays and their theory and measurements refer mostly to indoor environments. Therefore, this method is not appropriate to calculate the $WBGT_{SW}$, but it would be suitable for the calculation of the $WBGT_{LW}$.

Table 2 - Bernard's semi-empirical formula for T_{nwb} [31].

Criteria	**Equation**	**Ref. eq.**
$T_g - T_a > 4$ °C	$T_{nwb}=T_{pwb} + 0.25(T_g-T_a) + 0.1v^{1.1} - 0.2$	(8.1)
$T_g - T_a < 4$ °C; V > 3 m/s	$T_{nwb}=T_{pwb}$	(8.2)
Otherwise	$T_{nwb}=T_{pwb} – (0.96 + 0.069\log v) (T_a-T_{pwb})$	(8.3)

In addition, Lemke and Kjellstrom [30] have simplified the equations for calculating $WBGT_{LW}$. These are presented as eq. (9.1) and eq. (9.2) in Table 3.

Table 3 - Simplification for the calculation of $WBGT_{LW}$ [30].

Criteria	**Equation**	**Ref. eq**.
v > 3 m/s; $T_{nwb}=T_{pwb}$; $T_g=T_a$	$WBGT_{LW}=0.7T_{pwb}+0.3T_a$	(9.1)
0.03 m/s < v ≤ 3 m/s	$WBGT_{LW}=0.67T_{pwb}+0.33T_a-0.048\log v(T_a-T_{pwb})$	(9.2)

Liljegren et al. [32] used instead the heat exchange principles to calculate T_{nwb} and T_g. Since their equations for the calculation of the T_g involve both the diffuse and direct solar radiation, their method is mostly applied for clear as well as cloudy conditions. Additionally, the Liljegren et al. method includes all meteorological variables as required by the WBGT calculation. They compared the calculated $WBGT_{SW}$ and measured WBGT, and found that the differences were less than 1 °C for 95.0% of the time, except when the differences were attributed to equipment issues [30]. This method is preferred for calculating the $WBGT_{SW}$. Since Liljegren et al. have not

compared indoor measurements with the calculations of $WBGT_{LW}$, their method is not appropriate for the $WBGT_{LW}$.

A summary of the methodologies used in this research for calculations of the WBGT is presented in Table 4.

Table 4 - The methodologies used for different calculations of the wet bulb globe temperature.

Index	Solar radiation	Method based	Criteria	Air speed	Equation
WBGT	Long + short wave radiation	Liljegren	$T_g - T_a > 4$ °C	-	$WBGT_{SW}=0.7T_{nwb}+0.2T_g+0.1T_a$
	Only long wave radiation	Bernard	$T_g - T_a < 4$ °C	v > 3 m/s	$WBGT_{LW}=0.7T_{pwb}+0.3T_a$
				$0.03 < v \leq 3$ m/s	$WBGT_{LW}=0.67T_{pwb}+0.33T_a-0.048\log_{10}v (T_a-T_{pwb})$

3.1.6 Spatial mapping and Annual Radiation Heat Stress

The analysis space (i.e. office space) is framed with a grid of 0.5 x 0.5 m on the floor plan. The significance of the grid is to identify areas with the highest Annual Radiation Heat Stress (ARHS) percentage, where the manikin is exposed to extreme heat stress conditions (see Figure 4).

In this study, a similar approach to the ARD index, which is introduced by Zani et al. (2019) [17], is based on the WBGT variation (not ΔMRT variation) and named ARHS, is adopted to assess extreme heat stress conditions. The ARHS metric is defined as the percentage of the yearly-occupied hours when the ΔWBGT is positive for each manikin position (i.e. WBGT above the threshold of $WBGT_{ref}$). To define the WGBT, which is the $WBGT_{SW}$ or the $WBGT_{LW}$, the script refers to the threshold of 4 °C (see eq. (10)). The t_i is defined as each occupied hour in a year (h), and the $WBGT_i$ is the hourly value of wet bulb globe temperature (°C) for each point of the grid that will be compared with the threshold reference of WBGT for that specific hour.

$$ARHS = \frac{\sum_j (wf_i . t_i)}{\sum_j t_i} \quad wf_i = 1 \quad if; \quad WBGT_i > WBGT_{ref} \tag{10}$$

The ARHS metric is calculated based on the ΔWBGT, which creates an RGB mapping picture output. This can be used in the preliminary design stage by designers to show the distribution of the extreme heat stress conditions, which will be useful to assess different fenestration systems.

Additionally, in order to compare the differences caused by the effect of distance from the façade and the level of activity, it was decided to calculate the number of occupied discomfort hours, driven by solar radiation, that would occur for each of the test conditions if $\Delta WBGT > 0$.

3.2 Description of the test case scenario

The model replicates the ASHRAE BESTEST Lightweight office space [33], as it is considered a reference for indoor thermal comfort analysis. The model represents an office space, located in Milan (latitude 45.4642° N, longitude 9.1900° E), Italy. The dimensions of the office space are 8m in width, 6m in depth, and 3m in height. The south exposed façade holds two windows with dimensions of 2m x 3m each (see Figure 4). The hourly annual weather data was selected for Milano Linate 160800 IGDG from the Energy Plus Weather (EPW) repository [34].

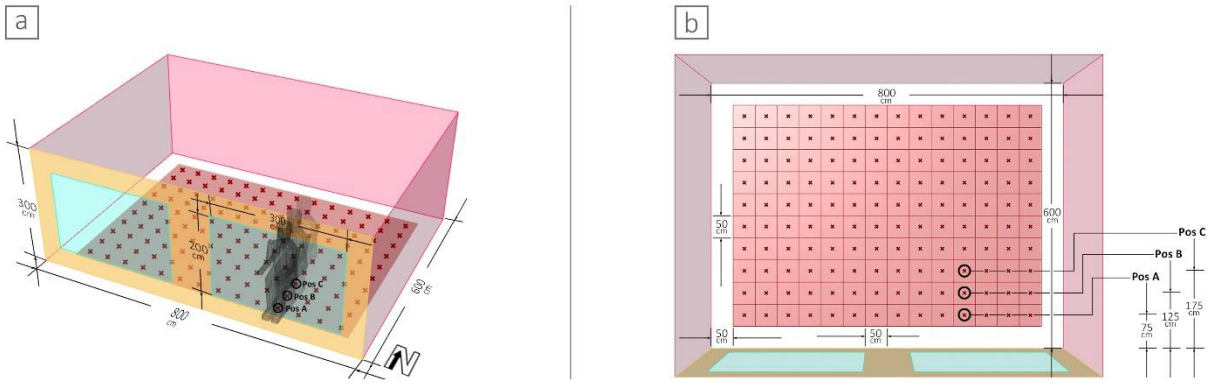

Figure 4 - a) Office space configuration with the analysis grid, and b) key plan with different positions of a manikin.

The thermal properties set for the elements composing the south-facing wall are listed in Table 5; all the other surfaces are considered to be adiabatic.

Table 5 - Exterior wall construction elements properties.

Element	**λ**	**x**	**U**	**ρ**	**C_p**
Unit	W/mK	m	W/m^2K	kg/m^3	J/kgK
Internal Surface Coefficient	-	-	8.290	-	-
Plaster Board	0.16	0.01	13.33	950	840
Fiber Glass Quilt	0.04	0.07	0.61	12	840
Wood Siding	0.14	0.01	15.56	530	900

External Surface Coefficient	-	-	29.30	-	-
Overall, air to air	-	-	0.51	-	-

Different alternatives are considered for the analysis in order to study the application of the WBGT approach for this case study with different envelope configurations: (1) the insulated glazing unit (IGU) with a T_{sol}=0.60 (T60), (2) the solar control glass with a T_{sol}=0.28 (T28), (3) the standard IGU plus Roller Blind with 0.3 solar transmittance overall (T60+R). The first two alternatives, the T60 and the T28, do not present shading systems, while the third alternative, the T60+R, presents a dynamic shading system. The roller blind is simulated as a translucent panel and it works according to the criteria defined with the sensor placed on the human body at the distance of 1.25 m from the window: if the $\Delta WBGT > 0$, the shading control is automatically on, otherwise, it is off. Meanwhile, the thermal and radiative properties set for the window and construction elements are summarized in Table 6.

Table 6 - Thermal and radiative properties of different elements.

Element	**U** (W/m^2K)	ρ_{sol} (-)	T_{sol} (-)
Exterior wall	0.51	0.5	-
Floor	Adiabatic	0.2	-
Ceiling	Adiabatic	0.8	-
Interior wall	Adiabatic	0.5	-
Glazing (1)	1.40	-	0.60
Glazing (2)	1.40	-	0.28
Shading	-	0.6	-

All the alternatives (T60, T28, and T60+R) are simulated by placing the manikin in three positions of 0.75 m, 1.25 m, and 1.75 m distant from the window in order to study the effect of the solar radiation on thermal comfort related to the distance from the fenestration system.

According to the office use, internal load density is defined as equipment (7 W/m^2), lighting (12 W/m^2) and people (0.05 people/m^2). The schedules of occupancy, equipment, and lighting are obtained accordingly from the default office schedules of Honeybee plug-in, taking into account 8:00 to 18:00 as working hours.

The case study was simulated under mechanically controlled indoor conditions to guarantee T_h=20 °C, T_c=26 °C with an ideal system with unlimited power able to instantaneously deliver the expected indoor thermal conditions. For the simulation, it was assumed that all windows were closed, the amount of infiltration was set to low, ~ 0.1 each, and air speed was considered to be 0.1 m/s.

Different metabolic rates were considered, those classified as resting, low metabolic rate, moderate metabolic rate and high metabolic rate. The M values were assigned according to the values listed in Table 1. These values were used for simulations of the occupied discomfort hours percentage, driven by solar radiation, to find the trend of this percentage against different metabolic rate values (increasing from very low to high metabolic rate). For the standard simulation, a low metabolic rate (e.g., 180 W) was set based on the office space.

To calculate hourly shortwave ΔMRT, the shortwave absorptivity was fixed for $\propto_{SW}$ = 0.67 (approximated value for white skin and average clothing). Likewise, the longwave absorptivity $\propto_{LW}$ of the human body was set to be approximately 0.95. The fraction of body surface exposed to radiation f_{eff} was set to be 0.696 (seated), h_r is the radiation heat transfer coefficient, which was assumed to be equal to 6.012 W/m^2 K, and the orientation of the manikins were toward the south. Finally, to compute WBGT, it was assumed that the office workers were always non-acclimatized in order to aim for the most unfavorable indoor thermal perception.

A comparative analysis was also performed for three specific days to better understand the effect of solar radiation on Adjusted MRT and WBGT (Section 4.4). The analysis was performed for the 1st to the 3rd of September, considering the maximum incident radiation (in Milan) that is on the 2nd of September at 11:00; this allowed monitoring of the trend of Adjusted MRT and WBGT with the presence of the incident solar radiation. These three days were selected to examine the sensitivity of WBGT, Adjusted MRT, and PMV, with the peak value of the incident solar radiation and to better study them for the largest solar radiation changes during these three days.

4 Results and discussion

The results from the simulations are broken down into five sections and represent examples of the typical outcomes obtained following the presented methodology. In Section 4.1, the annual analysis of indoor thermal comfort is presented. Section 4.2 presents the results of the occupied discomfort hours percentage, driven by solar radiation. Then, Section 4.3 explains the results of the ARHS metric. In Section 4.4, a comparison between ΔWBGT and Adjusted PMV is presented. In this section, detailed analysis for three days is also introduced to better study and interpret the presence of the solar radiation on the Adjusted MRT and WBGT. Section 4.5 presents the point-in-time values of predicted ΔWBGT and Adjusted PMV from the simulations. This part of the study

allows comparison of the results of the here presented approach with the outcome of the traditional thermal comfort model. It should be noted that all different sections of the outcomes are presented to show the potential of applying the proposed method under a variety of settings.

4.1 Annual analysis of indoor thermal comfort

In this section, annual heat maps of ΔMRT, ΔWBGT, and PMV are presented. Figure 5 shows the simulation results for T60 glazing with an occupant seated 0.75 m away from the window and facing the glazed surface. By considering the annual heat map of ΔMRT (see Figure 5a), large variations are found (values between 0 °C to 25 °C). By comparing annual heat maps of ΔMRT and ΔWBGT, it is evident that the latter highlights only severe heat stress conditions (see Figure 5a and c). This approach estimates the hourly WBGT values and compares them to the $WBGT_{ref}$ values, considering the correct metabolic rates, to find the heat stress conditions.

The annual map of the Adjusted PMV (Figure 5b) includes black dashed line patterns representing the conditions when Adjusted PMV values exceed the maximum validity range of the PMV scale (> +3). This means that it is certain that a heat stress condition is present, but the graph does not communicate this condition accurately because it neglects the criticality of the condition. Annual heat maps of Adjusted PMV and ΔWBGT give the possibility of preliminary comparison by qualitative means. WBGT provides a good estimation of the intensity of thermal heat stress through the color gradient used by revealing: (i) a less sensitive scale than PMV, (ii) a reduction of possible discomfort hours, and (iii) the capability of user adaptation.

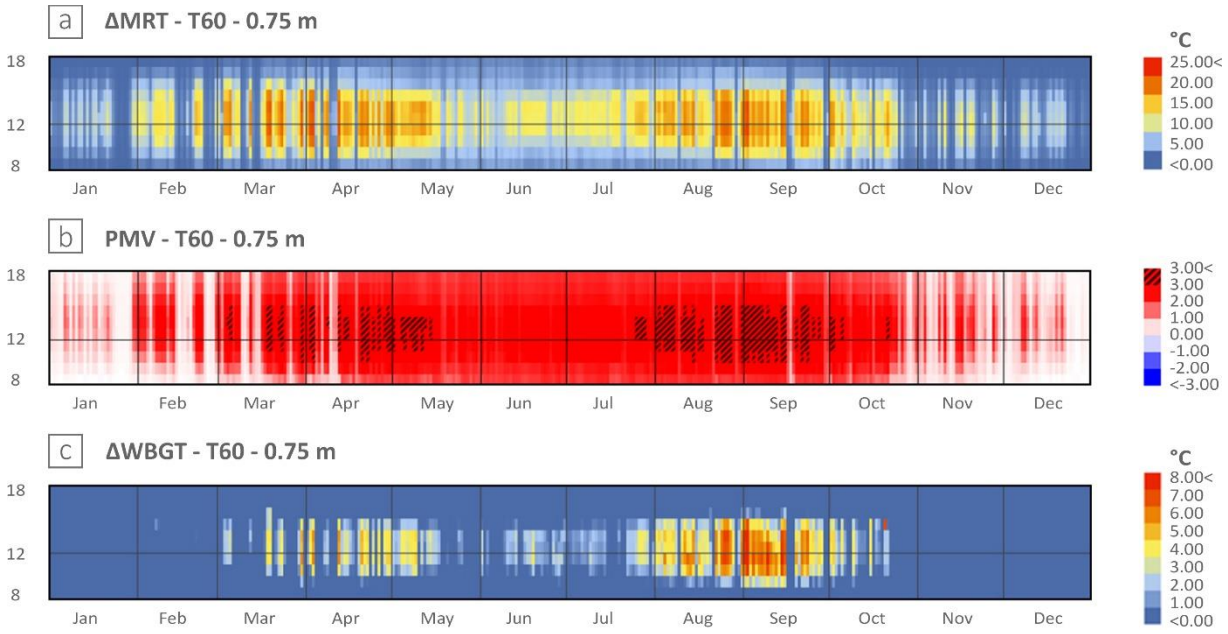

Figure 5 - Annual heat maps for T60, 0.75 m from the façade: a) ΔMRT, b) PMV, and c) ΔWBGT.

For the sake of comparison, additional results are presented. Figure 6 shows the results of three indices of ΔMRT, PMV and ΔWBGT for T28 glazing with an occupant seated 0.75 m away from the window and facing the glazed surface. Smaller variations in the annual heat map of ΔMRT (see Figure 6a) were found for this scenario compared to the T60 glazing scenario (see Figure 5a). The Figure 6b shows that Adjusted PMV values were between zero and three during working hours for the whole year. The ΔWBGT value was constantly zero, meaning that hourly WBGT value did not surpass the $WBGT_{ref}$ value all along the year (see Figure 6c). As the PMV, the WBGT is sensitive to the solar transmittance of the glazing, when estimating thermal discomfort in the indoor office environment. By comparing the PMV outcomes between the scenarios T60 and T28, the glazing with lower solar transmittance value did not show values outside the maximum threshold of the PMV (see Figure 5b and 6b). The ΔWGBT maps (Figure 5c and 6c) assert that risk of heat stress was avoided in the T28 scenario, while the extreme heat stress conditions (intensity and period) were highlighted in the T60 scenario due to the glazing used .

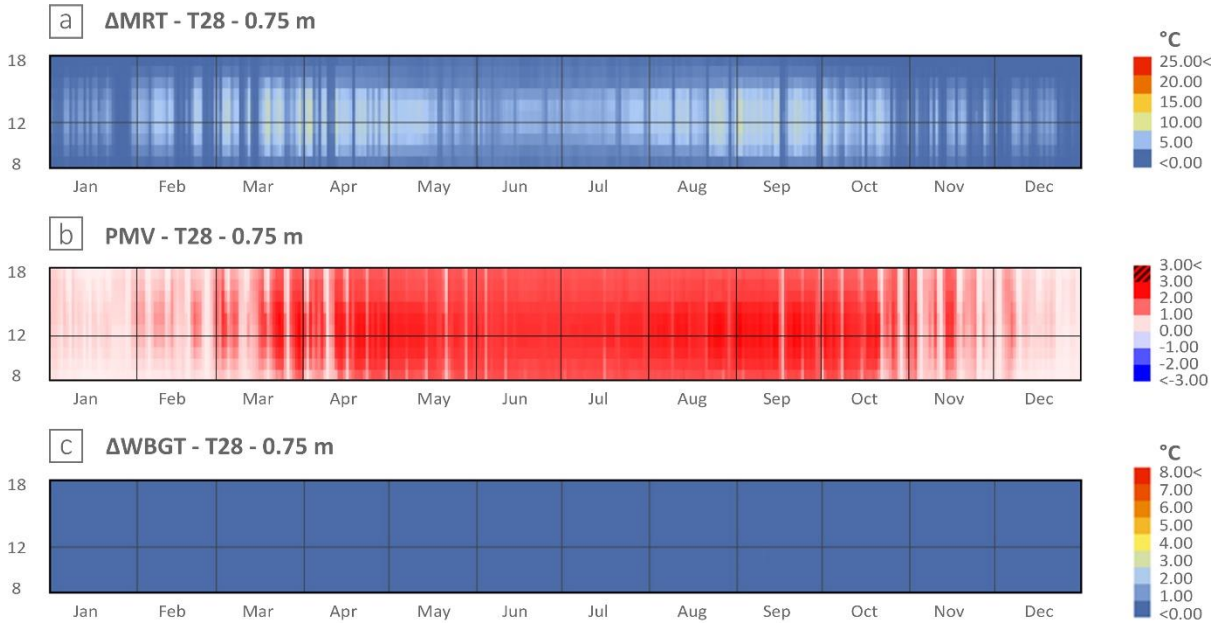

Figure 6 - Annual heat maps for T28, 0.75 m from the façade: a) ΔMRT, b) PMV, and c) ΔWBGT.

As it was found in the preliminary investigations described in Section 2.2, using the CBE Thermal Comfort Tool, the PMV value considering direct solar radiation can be above the maximum value of the thermal comfort scale (> +3). The comparison of the annual heat maps of Adjusted PMV and ΔWBGT presented in this section highlights that when the PMV exceeds the maximum range of the model in an extreme condition (see Figure 5b), it cannot well represent how warm the condition is perceived by the occupants. On the other hand, the WBGT approach can be seen as a better option, given that it is not only a less sensitive index, but also provides a good estimation of the heat stress condition taking into account the effect of the solar radiation.

4.2 Occupied discomfort hours percentage, driven by solar radiation

The occupied discomfort hours percentage, driven by the presence of the solar radiation, for different glazing types (T60 and T28), occupant positions (0.75 m, 1.25 m, and 1.75 m away from the window) and metabolic rates are compared in Figure 7a (during the working hours). This percentage was calculated in accordance with the value of WBGT that surpasses the limit boundaries of $WBGT_{ref,}$ for each of the assumed metabolic rates. Figure 7a summarizes the findings by counting the annual hourly conditions of heat stress for the scenarios T28 and T60 (figures 7b, c, and d). By assuming an increased level of activity from very low (e.g., resting with M=115 W) to very high activity (e.g., exercising with M=415 W), the risk of heat stress also rises. Since the body produces more heat internally, it experiences a higher body core temperature. For the scenario T60 at 0.75 m away from the window, the difference between the occupied discomfort hours percentage driven by solar radiation for a very low and very high level of activity inside the space was 35.0%. Due to the presence of direct solar radiation, there was a strong link between the perceived discomfort conditions and the transmittance of the glazing system. In the case of T28 at 0.75 m away from the window, the difference between the occupied discomfort hours percentage driven by solar radiation between a very low and very high level of activity was halved and decreased to 17.0%. Figures 7b, c, and d present the annual distribution of WBGT for three different positions 0.75 m, 1.25 m, and 1.75 m from the window for the scenario T60. Moving away from the window from 0.75 m to 1.75 m, a reduction of the calculated WBGT values that are positioned above the $WBGT_{ref}$ can be seen. For the scenario T60, 1.75 m away from the window, the general trend established was that from winter to summer, the values of WBGT were rising from 10 °C until 31 °C. This means that there was no condition above $WBGT_{ref}$ lines of 115 W, and consequently, the occupied discomfort hours percentage, driven by solar radiation, for this metabolic rate was zero. In winter, due to the lower altitude of the sun, the manikin (for both 0.75 m and 1.25 m from the window) received a greater amount of solar radiation. Whereas in summer, due to the higher altitude of the sun; only the area near the façade (0.75 m from the window) received a high amount of solar radiation. This does not mean that the manikin far from the window (1.75 m) did not represent a thermal discomfort condition, but it implies that the influence of direct solar radiation was reduced compared to the manikin closer to the window (0.75 m) and, the heat stress condition still can occur depending on other factors, (e.g., metabolic rate), defining the $WBGT_{ref}$ value.

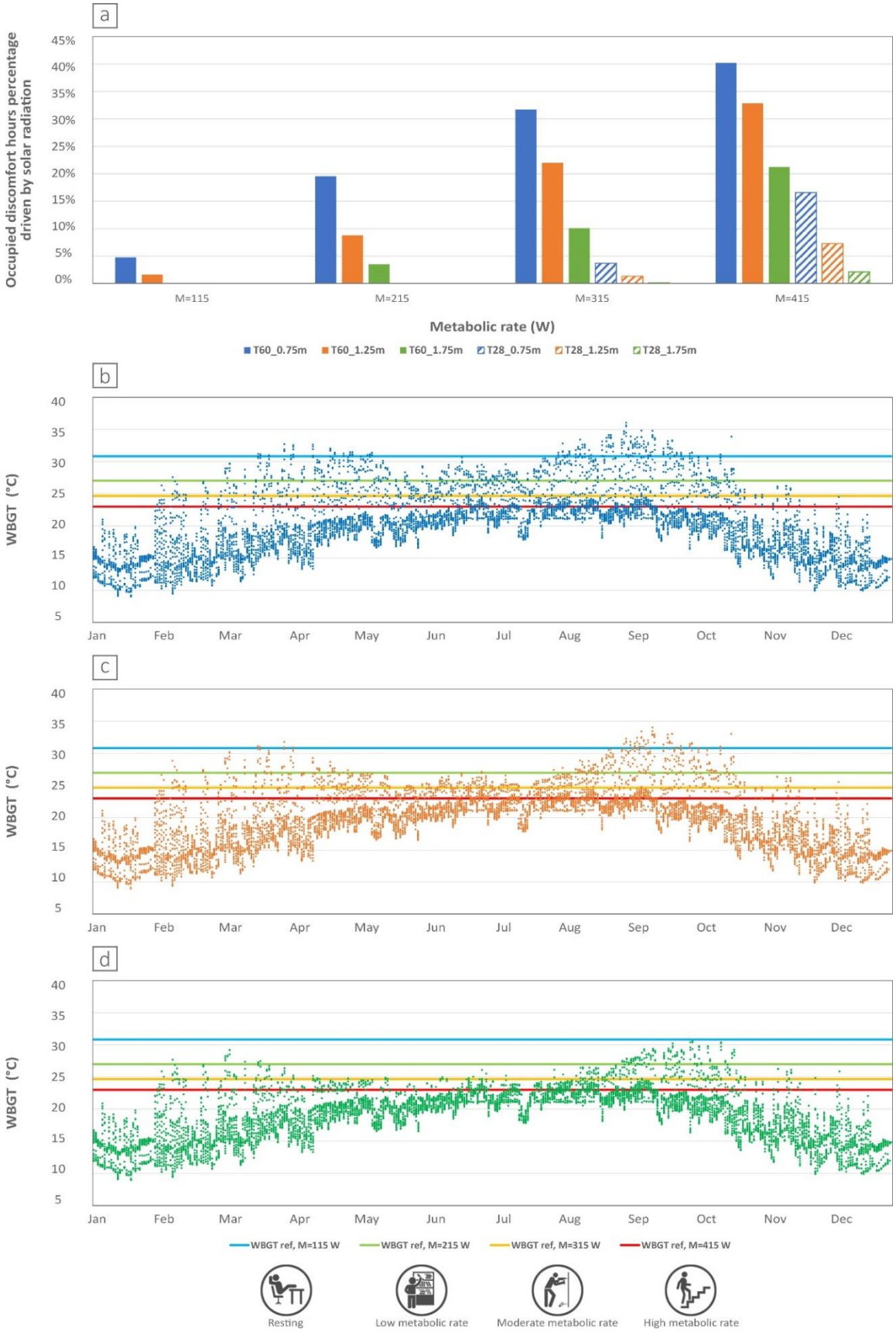

493

494 *Figure 7 - a) Occupied discomfort hours percentage, driven by solar radiation, and variation of WBGT during the year for*

495 *T60: b) 0.75 m, c) 1.25 m, and d) 1.75 m from the window.*

4.3 Annual Radiation Heat Stress

An example of a spatial map distribution of ARHS is hereby reported and is useful if it is based on the separation of manikins. This map shows the percentage of occupied discomfort hours; that is, where the ΔWBGT is greater than 0 °C. This map was created considering an increase in ΔWBGT (e.g., 1 °C) which corresponds to heat stress, under some particular condition (e.g. air temperature, metabolic rate), but it does not give an idea of the magnitude. Figure 8 shows the false-color plots of ARHS Autonomy for two different iterations, one without shading (T60) and the other considering a movable roller-shade (T60+R) for typical working hours in Milan (8:00-18:00).

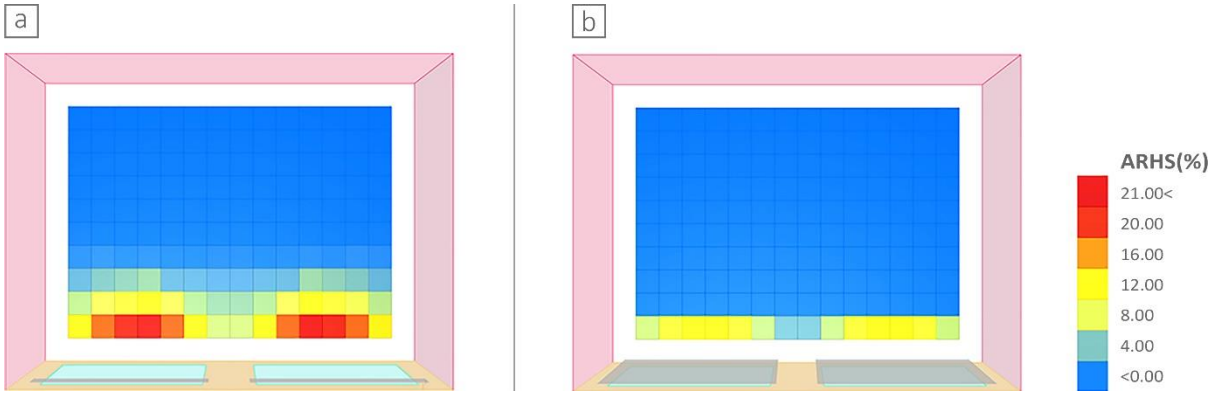

Figure 8 - False color plots of Annual Radiation Heat Stress with glazing a) T60, and b) T60+R.

The application of dynamic shading for the case of T60+R was made according to the criteria defined with the representative sensor (placed on the human body) at the distance of 1.25 m from the window and as described in the methodology chapter.

Due to the control strategy applied for the cases of T60+R (Figure 8b), lower annual radiation heat stress percentages were observed near the window than in the case of T60. It is visible from the plots for the case of T60+R that there is no area with ARHS > 12% because of the lower frequency of heat stress compared to the case of T60. Thus, the case of T60+R had a more favorable performance in terms of heat stress caused by solar radiation and a more flexible furniture plan for designing the interior space.

The metric of ARHS calculated using ΔWBGT can be a useful index for architects and designers to compare different fenestration systems, especially in the preliminary design stage, to reduce the effect of the incoming shortwave solar radiation. In a more holistic and detailed analysis, it can integrate in both daylight and energy simulations to address the trade-offs between all thermal and visual aspects for designing a more appropriate building envelope and shading devices systems.

4.4 Comparative analysis of indoor thermal comfort

A comparative analysis was performed for the 1st to the 3rd of September to better understand the effect of the solar radiation on Adjusted MRT and WBGT. The choice of the three days was made following the distribution of the change in the WBGT presented in Figure 7, in which can be seen a peak in heat stress due to the coupled effects of temperature, solar radiation intensity, and solar altitude (and related solar access). Significant variations on the WBGT were found, with a considerable hourly fluctuation of the value during the day, and in particular at midday. The maximum value of Adjusted MRT for this period was 51 °C, while the value of WBGT reached up to 32 °C, coupled both with an indoor air temperature equal to 26 °C (considering the distance of 1.25 m from the window). As expected, in Figure 9 it is shown that the value of Adjusted MRT was often higher than the MRT. For example, on the 2nd of September at 12:00, ΔMRT reached 17 °C (Figure 9a and b).

Figure 9c also compares the hourly values of Adjusted PMV (including the intensity of the shortwave solar radiation on the occupant) with ΔWBGT for the case of T60, for different positions away from the window for the selected analysis period. For the worst condition (i.e. the 2nd of September at15:00, for the case of 0.75 m away from the window), the Adjusted PMV reached a +4 thermal sensation scale, which exceeded the limits of its standard seven-point scale, while the WBGT remained under the maximum limit (Figure 3). Consequently, the WBGT was within the boundary thresholds, while the Adjusted PMV was not. The Bernard and Liljegren tags on the horizontal axis of Figure 9c show the period that each of the methods was used to estimate the hourly WBGT value, which is compared with the $WBGT_{ref}$ for calculating ΔWBGT. For instance, the Liljegren methodology was used with the presence of solar irradiance during midday, while there are conditions that the Bernard method was implemented due to the absence of the solar irradiance.

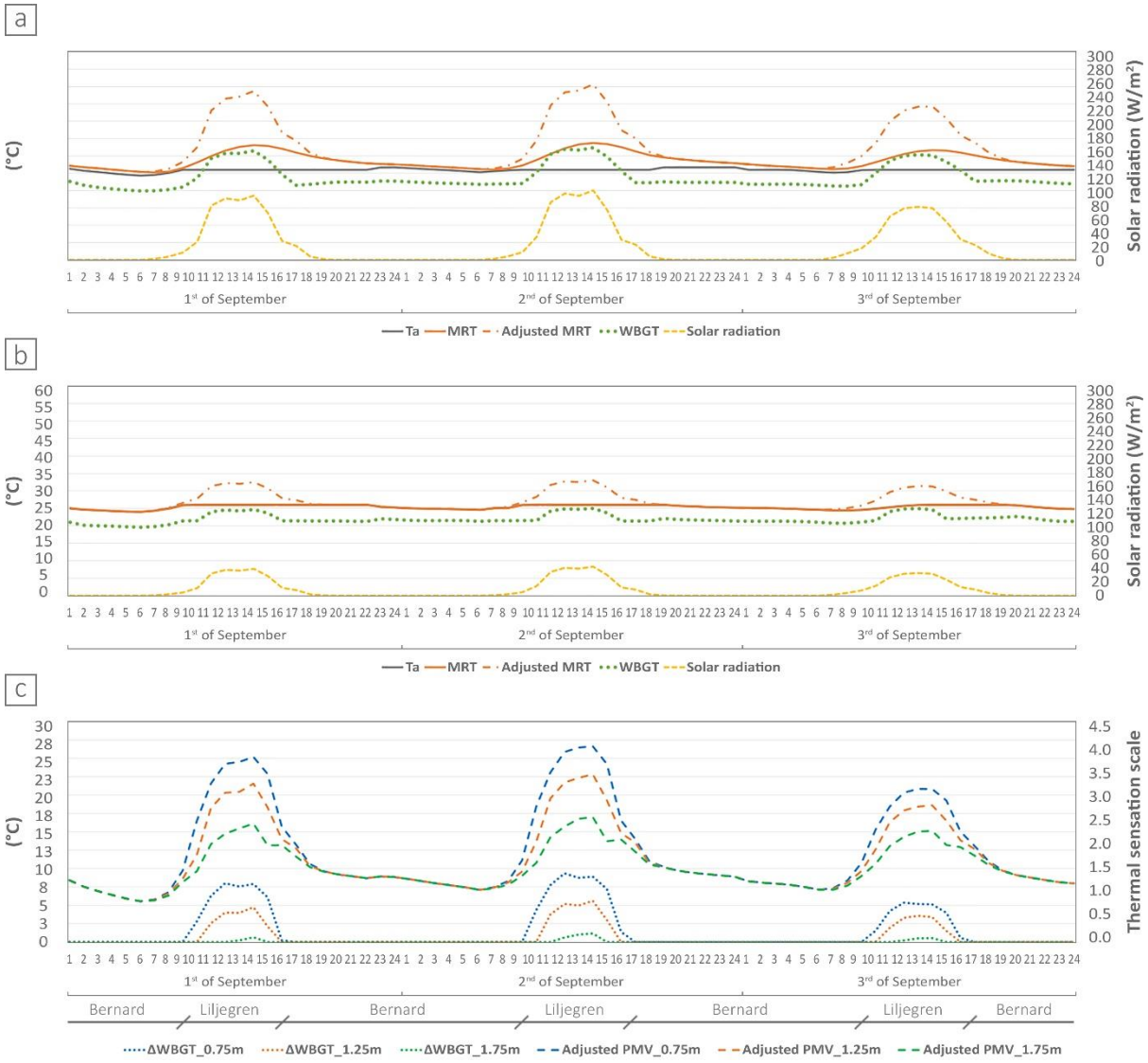

538

539 *Figure 9 - a) Comparative analysis of air temperature, MRT, Adjusted MRT, WBGT, and Solar radiation from the 1st to the*
540 *3rd of September, 1.25 m from the window for T60, b) comparative analysis of air temperature, MRT, Adjusted MRT, WBGT,*
541 *and Solar radiation from the 1st to the 3rd of September, 1.25 m from the window for T28, and c) the effect of user distance*
542 *from the façade on ΔWBGT and Adjusted PMV from the 1st to the 3rd of September, for T60.*

543 The detailed hourly results presented in this section show that the WBGT, such as Adjusted PMV, is sensitive to
544 the position of occupant and the material's properties of the building envelope, especially the solar transmittance
545 value of the glazing, and can be used to estimate the dissatisfaction in the indoor office environment.
546 Comparative analysis of indoor thermal comfort proves that the Adjusted PMV value could be higher than the
547 maximum acceptable value of PMV for some extreme conditions. However, given that it is a less sensitive index
548 to huge solar radiation change, the heat stress index of WBGT can be seen as a better option to assess the direct
549 solar radiation effect and s, to smooth the out of scale values by limiting their intensity. The time span of hours

for assessing the discomfort is reduced using this approach, but the peak intensity is overlapping for both ΔWBGT and Adjusted PMV, and the resulting values are out of the validity limit of the formula.

It should be noted that the heat stress approach does not express the general comfort condition of occupants inside the space. As an aim of this study was the assessment of the presence of the direct solar radiation effect, it has been considered only for the dissatisfaction mostly caused by shortwave solar radiation. However, further improvements are needed to take the thermal comfort hours and their overlapping with heat stress hours into account in the design stage. These developments will help to inform the design process and provide designers with better insight for improving the performance of building envelope leading to the creating of office environments that are more thermally comfortable and positively affect the occupants' productivity.

4.5 Point-in-time predicted ΔWBGT and Adjusted PMV

This last section of results is presented to highlight the differences between predicted ΔWBGT and Adjusted PMV considering several point-in-time simulation results. Table 7 gives the prediction of WBGT and ΔWBGT values corresponding to particular combinations of the parameters (e.g. ERF, relative humidity, air temperature, MRT, Adjusted MRT). These results are presented considering 0.1 m/s as air speed, 180 W (1.7 met) as metabolic rate and 0.6 clo as clothing level.

Table 7 - Examples of prediction of WBGT, ΔWBGT, and Adjusted PMV from the simulations.

Condition	ERF (W/m^2)	RH (%)	T_a (°C)	MRT (°C)	ΔMRT (°C)	Adjusted MRT (°C)	WBGT (°C)	ΔWBGT (°C)	Adjusted PMV
(1)	28.3	30.4	21.6	21.0	6.8	27.8	18.8	0.0	0.1
(2)	57.0	21.3	26.0	26.0	13.7	39.7	25.4	0.0	1.6
(3)	89.0	39.3	26.0	31.0	21.3	52.3	31.1	3.0	3.3
(4)	94.0	55.0	26.0	32.7	22.5	55.2	35.6	7.5	4.0

Table 7 presents multiple examples of point-in-time values from the results of the simulation. Conditions (1) and (2) are presented for the combinations of parameters that yield values of 0.1 and 1.6 on the thermal sensation scale, respectively. The prediction of the WBGT heat stress model for these conditions was zero due to low incident solar radiation combined with other parameters.

The outcomes of the traditional PMV model considering the Adjusted MRT values of 52.3°C condition (3) was 3.3 on the thermal sensation scale (PMV > +3). This condition shows that for this point-in-time, the PMV model was unable to express how much heat iin this condition was caused by the 89.0 W/m^2 ERF value, with 52.3 °C Adjusted MRT. With reference to the traditional PMV model, it is not possible to interpret the difference between 3.3 for condition (3) and 4.0 for condition (4) in terms of thermal sensation scale. It should be noted that the WBGT > 31.1 is almost equal to PMV > +3: this implies to have missing information about the magnitude of the heat stress.

The ΔWBGT approach clearly states that when the value of WBGT is higher than $WBGT_{ref}$, it is a condition with heat stress (e.g., ΔWBGT value of 3.0 °C for the conditions (3)); otherwise, there is no heat stress (e.g., ΔWBGT value of zero for the conditions (1) and (2)).

The PMV model predicts the thermal comfort condition of occupants with the ASHRAE seven-point thermal sensation scale (cold, cool, slightly cool, neutral, slightly warm, warm, and hot), and as long as incident solar radiation is low or absent, this prediction can be reasonable. However, its value falls out of scale in the presence of shortwave solar radiation (extreme events). Moreover, human beings are not always able to perceive the heat stress, nor the changes. The alternative method of WBGT is pretty similar to the PMV model, where there is the presence of shortwave solar radiation effects. However, the WBGT has the capability to consider the user adaptation by reducing the number of conditions perceived as a heat stress.

The heat stress approach of WBGT does not classify the thermal comfort conditions as neutral, slightly warm, etc., but identifies the heat stress based on the pre-defined threshold and further quantifies this heat stress with a WBGT value. From this perspective, the use of WBGT, which makes the heat stress determination less sensitive to solar radiation values and reduces out of scale values, is preferable for the purpose of evaluating the effect of solar radiation on indoor thermal comfort.

5 Limitations of the study

This section presents some limitations of this study that might encourage future developments. Firstly, the air speed inside the indoor environment was considered constant, given that the focus of this study was to demonstrate the application of the WBGT approach in assessing the direct solar radiation effect on indoor thermal comfort. Linking CFD simulation results on air velocity with the proposed methodology might help to predict more realistic heat stress conditions.

Secondly, the reflected radiation from the surrounding surfaces (e.g., walls, ceiling and floor) has already been assessed by means of the simulation procedure, enabled by the Radiance - DC method, estimating the amount of irradiation directly falling on the manikin and the amount of reflected portion from the rooms' surfaces toward the manikin. A standard office, with average surface solar reflectances for the surfaces, was proposed in this study. Further dedicated analysis should be conducted to quote specifically how the change in reflectance of each internal surface, or the average reflectance of the room surfaces can affect the thermal comfort perceived by the user.

Thirdly, in relation to the Radiance - DC method, the modeled geometry and manikin considered do not include a desk as a working plane for the occupant, which would represent an immediate shading source, thereby changing the total solar radiation falling on the occupant, and the re-reflected component of solar radiation might also increase the intensity of total solar radiation. Adding desks to the analysis scene would allow thorough and precise calculation of the solar radiation landing on the human body could be reached. In this way, all the critical aspects, from the overshadowing effect to solar reflections, could be considered. However, furniture surfaces are mostly unknown to the designer.

Fourthly, the value of f_{eff} (which in the standardized calculation includes overshadowing effects and the effect of clothing for incident solar radiation reduction) can lead to a change in ΔMRT of up to 30%. The exposure may be different depending on the way the manikin is placed, but it is an approximation. It should be mentioned that this assumption does not directly affect the WBGT and ΔWBGT results (change in WBGT up to 5%). More in-depth analysis is needed in subsequent work to take into account this limitation.

Fifthly, regarding the WBGT heat stress approach, it does not express the general comfort condition of occupants inside an indoor space. Consequently, in order to better understand the thermal comfort together with the heat stress conditions, an integrated approach can be developed in the future. The approach allows an overall insight on how the designers' decisions directly affect the building envelope choices toward the definition of high-performance office environments.

Finally, the WBGT calculation has several steps. Hence, future work can foresee a user-friendly software to be used in the preliminary design stage by the architects and designers. Moreover, this WBGT methodology will be potentially applicable as a heat stress index for both indoor and outdoor conditions. Consequently, it can be used with a similar procedure to assess outdoor comfort in a future study.

6 Conclusions

This research introduces a framework to assess the effect of incoming shortwave solar radiation on indoor thermal comfort and estimates the perceived thermal stress of the occupants. The novelty of this study is that it demonstrates the implementation of the WBGT heat stress index for indoor thermal comfort through the evaluation of the effect of solar radiation using the Radiance - DC method on the Grasshopper platform. This framework is used to assess the discomfort hours due to shortwave solar radiation landing directly on occupants considering it as heat stress by computing the ΔWBGT. To do so, two procedures are available to compute the WBGT: the equation proposed by Bernard, which is used to assess the effects of longwave solar radiation, and Liljegren's equations, which account for long and shortwave radiation. The results show the potential of applying the proposed method under a variety of settings. For instance, the Liljegren methodology can be used with the presence of solar irradiance during midday, while there are conditions with an absence of solar irradiance for which the Bernard method can be implemented .

The PMV is the most widely used thermal comfort perception index. The way that the laboratory tests are carried out and make it particularly sensitive when the person is exposed to direct solar radiation. The values that fall out of the scale are not able to express the perceived heat stress properly. The WBGT has been tested as an alternative, and the methodology is preferred, being less sensitive to huge solar radiation changes, reducing the out of scale values, and limiting their expression of intensity.

The ARHS metric is similar to the ARD index, but it is based on the WBGT approach. The ARHS metric uses WBGT to soften the sensitivity. It is applicable either indoor or outdoor, and it is flexible for rapid calculation on spatial analysis. The spatial heat stress conditions across the indoor space can be assessed and compared for different fenestration systems to reduce the effect of incoming shortwave solar radiation.

The detailed WBGT approach is potentially applicable for indoor environments under a variety of conditions, as it was already reported in the literature for indoor thermal comfort. However, this study stresses this approach by introducing a Delta Value approach that is based on Radiance - DC method. The proposed approach allows designers, architects, and energy modelers to predict the heat stress of occupants across the area for every hour of the year. The solar radiation can have an impact on the user's thermal perception onto a warmer condition, which can cause a comfortable or an uncomfortable state depending on the combination of indoor environmental parameters. Even though the direct solar radiation landing on the occupant may occur only a few hours a day, it can also be reflected from the surroundings and can significantly change the perception of the occupant (see Figure 9). The excess heat produced by shortwave solar radiation cannot be compensated for a standard HVAC system, depending on air velocity, air temperature, and air-outlets location. This may modify and, most probably, increase

656 the hours of discomfort experienced by the occupants, leading to decreased human health, well-being, and,
657 subsequently, productivity in an office.

658

659 References

660 [1] ASHRAE, *Handbook of Fundamentals*. 2013.
661 [2] Y. Al Horr, M. Arif, A. Kaushik, A. Mazroei, M. Katafygiotou, and E. Elsarrag, "Occupant productivity
662 and office indoor environment quality: A review of the literature," *Build. Environ.*, vol. 105, pp. 369–389,
663 2016.
664 [3] M. B. C. Aries, J. A. Veitch, and G. R. Newsham, "Windows , view , and office characteristics predict
665 physical and psychological discomfort," *J. Environ. Psychol.*, vol. 30, pp. 533–541, 2010.
666 [4] ANSI/ASHRAE, "ASHRAE Standard 55, Thermal Environmental Conditions for Human Occupancy,"
667 2017.
668 [5] K. Ceria and R. De Dear, "Thermal comfort and behavioural strategies in office buildings located in a
669 hot-arid climate," *J. Therm. Biol.*, vol. 26, pp. 409–414, 2001.
670 [6] P. O. Fanger, *Thermal comfort. Analysis and applications in environmental engineering*. 1970.
671 [7] BSI, "BS EN ISO 7730: 2005 - Ergonomics of the thermal environment–Analytical determination and
672 interpretation of thermal comfort using calculation of the PMV and PPD indices and local thermal comfort
673 criteria," 2005.
674 [8] S. I. H. Gilani, M. H. Khan, and W. Pao, "Thermal comfort analysis of PMV model Prediction in Air
675 conditioned and Naturally Ventilated Buildings," *Energy Procedia*, vol. 75, pp. 1373–1379, 2015.
676 [9] R. J. de Dear and G. Brager, "Developing an Adaptive Model of Thermal Comfort and Preference," 1998.
677 [10] BSI, "BS EN 16798 - 1: 2019 - Tracked Changes - Energy performance of buildings - Ventilation for
678 buildings," 2019.
679 [11] F. Bauman and E. Arens, "Task / Ambient Conditioning Systems : Engineering and Application
680 Guidelines," 1996.
681 [12] E. Arens, T. Hoyt, X. Zhou, L. Huang, H. Zhang, and S. Schiavon, "Modeling the comfort effects of short-
682 wave solar radiation indoors," *Build. Environ.*, vol. 88, pp. 3–9, 2015.
683 [13] C. Marino, A. Nucara, M. Pietrafesa, and E. Polimeni, "The effect of the short wave radiation and its
684 reflected components on the mean radiant temperature: modelling and preliminary experimental results,"
685 *J. Build. Eng.*, vol. 9, pp. 42–51, 2017.
686 [14] A. Zani, A. G. Mainini, J. D. B. Cadena, S. Schiavon, and E. Arens, "A New Modeling Approach for the
687 Assessment of the Effect of Solar Radiation on Indoor Thermal Comfort," in *Building Performance*
688 *Analysis Conference and SimBuild*, 2018.
689 [15] H. Zhang, E. Arens, and C. Huizenga, "Thermal sensation and comfort models for non-uniform and
690 transient environments, part III: Whole-body sensation and comfort," *Build. Environ.*, vol. 45, pp. 399–
691 410, 2009.
692 [16] C. Huizenga, Z. Hui, and E. Arens, "A model of human physiology and comfort for assessing complex

thermal environments," *Build. Environ.*, vol. 36, no. 6, pp. 691–699, 2001.

[17] A. Zani, H. David Richardson, A. Tono, S. Schiavon, and E. Arens, "A simulation-based design analysis for the assessment of indoor comfort under the effect of solar radiation," in *SimAUD*, 2019, pp. 135–142.

[18] S. Carlucci, F. Causone, F. De Rosa, and L. Pagliano, "A review of indices for assessing visual comfort with a view to their use in optimization processes to support building integrated design," *Renew. Sustain. Energy Rev.*, vol. 47, pp. 1016–1033, 2015.

[19] A. Beizaee, K. Vadodaria, and D. Loveday, "Assessing the ability of PMV model in predicting thermal sensation in naturally ventilated buildings in UK," in *7th Windsor Conference: The changing context of comfort in an unpredictable world*, 2012.

[20] S. Schiavon, T. Hoyt, and A. Piccioli, "Web application for thermal comfort visualization and calculation according to ASHRAE Standard 55," *Build. Simul.*, vol. 7, pp. 321–334, 2014.

[21] T. Hoyt, S. Schiavon, A. Piccioli, T. Cheung, D. M. And, and K. Steinfeld, "CBE Thermal Comfort Tool." 2017.

[22] E. Naboni, E. Danzo, and L. Ofria, "A Parametric Workflow to Concieve Facades as Indoor and Outdoor Climate," in *SimAUD*, 2019.

[23] F. R. d'Ambrosio Alfano, B. I. Palella, and G. Riccio, "Thermal Environment Assessment Reliability Using Temperature — Humidity Indices," *Ind. Health*, vol. 49, 2011.

[24] Z. Zamanian, Z. Sedaghat, M. Hemehrezaee, and F. Khajehnasiri, "Evaluation of environmental heat stress on physiological parameters," *J. Environ. Heal. Sci. Eng.*, vol. 15, pp. 1–8, 2017.

[25] K. Blazejczyk, Y. Epstein, G. Jendritzky, H. Staiger, and B. Tinz, "Comparison of UTCI to selected thermal indices," *Int. J. Biometeorol.*, vol. 56, pp. 515–535, 2012.

[26] R. McNeel, "Grasshopper generative modeling for Rhino." 2010.

[27] BSI, "BS EN ISO 7243: 2017 - Ergonomics of the thermal environment - Assessment of heat stress using the WBGT (wet bulb globe temperature) index," 2017.

[28] BSI, "BS EN ISO 8996: 2004 - Ergonomics of the thermal environment - Determination of metabolic rate," 2004.

[29] F. R. D'Ambrosio Alfano, J. Malchaire, B. I. Palella, and G. Riccio, "WBGT index revisited after 60 years of use," *Ann. Occup. Hyg.*, vol. 58, pp. 955–970, 2014.

[30] B. Lemke and T. Kjellstrom, "Calculating workplace WBGT from meteorological data: a tool for climate change assessment.," *Ind. Health*, vol. 50, pp. 267–78, 2012.

[31] T. E. Bernard and M. Pourmoghani, "Prediction of Workplace Wet Bulb Global Temperature," *Appl. Occup. Environ. Hyg. ISSN*, vol. 14, 1999.

[32] J. C. Liljegren, R. A. Carhart, P. Lawday, S. Tschopp, and R. Sharp, "Modeling the Wet Bulb Globe Temperature Using Standard Meteorological Measurements," *J. Occup. Environ. Hyg.*, vol. 5, pp. 645–655, 2008.

[33] R. H. Henninger and M. J. Witte, "EnergyPlus testing with ANSI/ASHRAE standard 140-2001 (BESTEST)," Washington, D.C., 2001.

[34] "Energy Plus Weather Data," *EnergyPlus*. [Online]. Available: https://energyplus.net/weather.